NAZARBAYEV UNIVERSITY

SPATIOTEMPORAL ORGANIZATION OF FOCAL ADHESIONS IN MIGRATING CELLS

ARINA ZHURAVEL

(B.Sc., Nazarbayev University)

A THESIS SUBMITTED IN PARTIAL FULFILMENT OF THE REQUIREMENT OF NAZARBAYEV UNIVERSITY FOR THE DEGREE OF MASTER OF SCIENCE IN BIOLOGICAL SCIENCES AND TECHNOLOGIES

APRIL 2024

Student: Arina Zhuravel  24 April 2024

Student's Supervisor: Ivan Vorobyev  24 April 2024

EXAMINERS

The M.Sc. thesis of Arina Zhuravel has been approved by the examiners.

Dr. Gonzalo Hap Hortelano, PhD, School of Sciences and Humanities, Nazarbayev University

Dr. Dana Akilbekova, PhD, School of Engineering and Digital Sciences, Nazarbayev University

DECLARATION

I hereby declare that this thesis is my original work, and it has been written by my in its entirety.
I have duly acknowledged all the sources of information which have been used in the thesis.
This thesis has also not been submitted for any degree in any university previously.

Arina Zhuravel

26 April 2024

ACKNOWLEDGEMENTS

To my supervisor Dr. Ivan Vorobyev, for his invaluable mentorship throughout the development of this thesis project.

To lab members Dr. Aleena Saidova, Vadim Mustyatsa, Aisulu Anapina, Madina Tlegenova, Nurdaulet Kulsharip, Iliyas Marat who have actively contributed to this project.

To Dr. Sholpan Kauanova, who was my first tutor in wet lab work.

To my family and friends for being my unwavering support system.

TABLE OF CONTENTS

ABSTRACT

Focal adhesions (FAs) are pivotal integrin-based macromolecular assemblies that orchestrate cell migration through traction force transmission by connecting cytoskeleton to extracellular matrix (Legerstee & Houtsmuller, 2021). While substantial progress has been made in understanding of the regulation of cell motility (Merino-Casallo et al., 2022), it remains elusive how considerable FA heterogeneity correlates with regional requirements to substrate adhesions intrinsic to cell migration. To evaluate FA dynamics, we employed live cell time-lapse microscopy with high spatial and temporal resolution, tracking FA size, lifetime, and intensity in cancer A549 cell line stably expressing Vinculin-RFP. We observed numerous small, short-living adhesions at the leading edge, which had formed both at large lamellae aligning with the vector of cell body translocation and smaller lateral lamellae. That contrasted with the presence of only a few large adhesions at the trailing edge. While FA maturation at the leading edge in response to tension generated by myosin II-decorated actin stress fibers has already been described, the origin of large FAs at the trailing edge remains poorly elucidated (Choi et al., 2008). Most FAs present at the trailing edge originated within lateral protrusions and only few of them formed directly there. During retraction of the trailing cell edge, a portion of FAs has already been disassembled before retraction has reached them. However, some FAs at the trailing edge were enlarging, either through merging with neighboring FAs or gradual increase in area and intensity as they slid along with the trailing edge relative to the substrate. As a result, relatively large FAs were forcibly detached and rapidly disassembled only upon retraction edge reached them. In summary, FA formation and maturation exhibited regionally regulated dynamics, and disassembly of FAs at the rear edge before retraction was not a prerequisite to edge retraction.

LIST OF TABLES AND FIGURES

disassembly, Oscillation – FAs with oscillations in integral brightness and length. n = 147 FAs, 10 cells. Kruskal-Wallis test, Dunn's multiple comparisons revealed no significant differences between groups.

Figure 10. *Left*: Formation of a cluster at the leading edge through merging of two individual FAs. *Right***:** Cluster splitting into two daughter FAs. Scale bar: 5 μm.

Figure 11. Cluster formation frequency (%) relative to the total formation events (clusters and individual FAs included). Clusters were notably more frequent at the trailing edge (47%) than at the leading edge (6%). n=15 in each group. Mann-Whitney test, ***p<0.001.

Figure 12. Cluster and individual FA formation density (events/100 um^2/10 min). Kruskal-Wallis test, Dunn's multiple comparisons. *p<0.05, **p<0.01, ***p<0.001.

Figure 13. The scheme of a basic cluster tree, displaying merging of two individual FAs and subsequent splitting of a cluster into two daughter FAs. The lifetime of this cluster is 12 min.

Figure 14. Lifetimes of individual FAs (iFA) and clusters at the leading edge (LE) and trailing edge (TE) of A549 cells, n = 150 FAs of each type, 10 cells. Kruskal-Wallis test, Dunn's multiple comparisons. **p<0.01, ***p<0.001.

Figure 15. Forced retraction of FAs at the trailing edge in migrating A549 cell (green and cyan arrows). posterior protrusion generating new FAs at the trailing edge (yellow ellipses). Interframe interval 2 min. Scale bar: 20 um.

Figure 16. Color-coded time-lapse of A549 cell migration. Dynamic migration of is depicted over time, visually coded from blue (older) to red (newer regions) using a rainbow spectrum corresponding to the duration of the time-lapse recording (30 min). Both leading and trailing edges are clearly distinguishable. Scale bar: 15 μm. The figure was created with the Time Lapse Color Coder plugin in ImageJ.

Figure 17. Lifetimes of FAs that translocated for more than 1 μm (n = 84) and that were stationary (n = 68) in A549 cell line, 5 cells. Kruskal-Wallis test, Dunn's multiple comparisons. *** p<0.001.

ABBREVIATIONS

A549 – human lung adenocarcinoma cell line

Arp2/3 – Actin-related Protein complex

ATCC – American Type Culture Collection

CMOS – complementary metal-oxide semiconductor

DMEM – Dulbecco's Modified Eagle Medium

ECM – extracellular matrix

FA – focal adhesion

FAK – focal adhesion kinase

FBS – fetal bovine serum

ICAM-1 – Intercellular cell adhesion molecule-1

iFA – individual focal adhesion

iPALM – interferometric photoactivated localization microscopy

LDV – extracellular matrix amino acid sequence Leu-Asp-Val

LE – leading edge

MAdCAM-1 – Vascular cell adhesion molecule-1

MT – microtubules

RFP – red fluorescent protein

RGD – extracellular matrix amino acid sequence Arg-Gly-Asp

TE – trailing edge

VASP – Vasodilator-stimulated phosphoprotein

VBS – Vinculin-binding site

VCL – vinculin

1. INTRODUCTION

Cell migration is a fundamental process underlying both normal development and pathological processes such as tumor metastasis (Friedl & Gilmour, 2009; Maziveyi & Alahari, 2017; Scarpa & Mayor, 2016). The initiation of a classic processive motility cycle occurs as a polarized cell extends a protrusion of the leading edge, driven by actin polymerization (Mattila & Lappalainen, 2008). Following this, the protruded edge stabilizes as it adheres to the substrate via cell-extracellular matrix (ECM) adhesions. These adhesions establish traction sites for propulsive forces that propel the cell forward. Further, myosin motors generate a contractile response of the actomyosin complex, which leads to the rapid formation of bundles of actin filaments (stress fibrils), which connect distal adhesions, resulting in strain of the cell body on the substrate and the cell body spreads out and moves forward (Ridley et al., 2003). The final phase of the migration cycle involves the retraction of the cell's rear end by releasing the adhesions (**Fig. 1**). Deregulation of cell adhesion and migration are implicated in tumorigenesis and are recognized as significant drivers of metastatic tumor progression (Rooney et al., 2010).

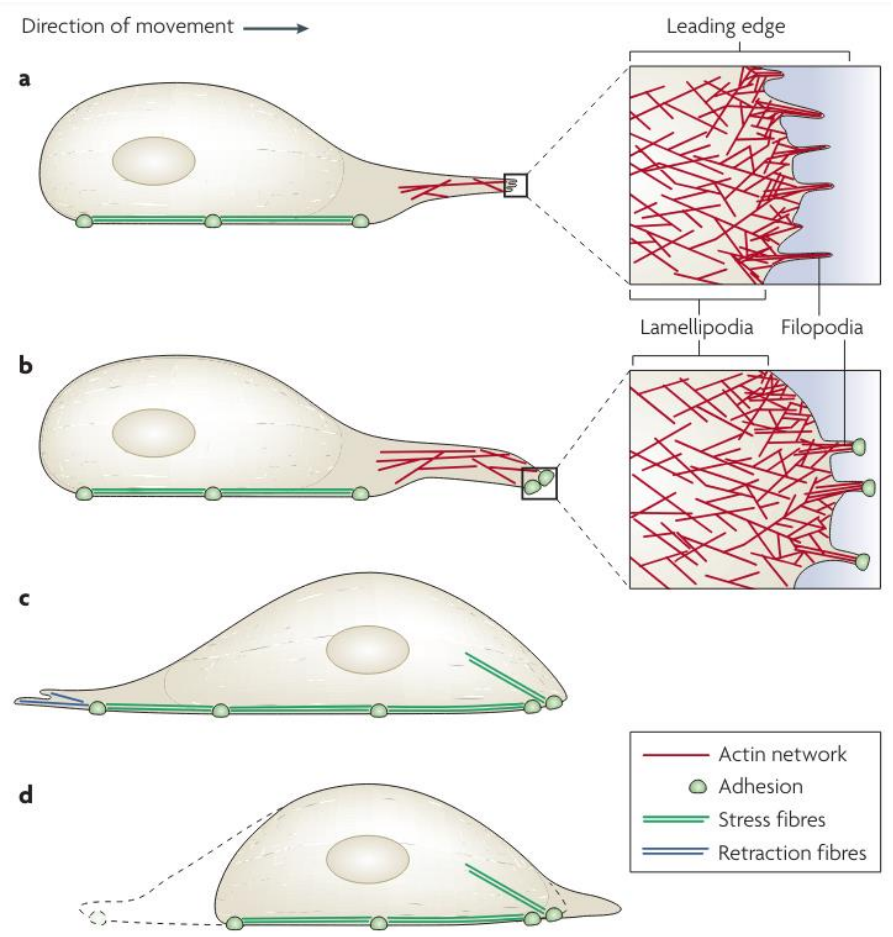

Figure 1. Cell body translocation depends on actomyosin contractility and cell-extracellular matrix adhesions (Mattila & Lappalainen, 2008)

1.1 Structure of focal adhesions

Central to cell migration are focal adhesions (FAs), integrin-based complexes that connect the cytoskeleton to the extracellular matrix (ECM) and provide traction force necessary for cell motility as well as signal transduction (Geiger et al., 2001; Legerstee & Houtsmuller, 2021; Prager-Khoutorsky et al., 2011). FAs emerge as crucial players in cellular migration across diverse migration models, encompassing both *in vitro* and *in vivo* contexts in both two- and three-dimensional (2D and 3D) environments (Cukierman et al., 2001; Harunaga & Yamada, 2011, Yamada & Sixt, 2019).

The formation of a focal adhesion begins when the integrin receptor is activated by ECM proteins, which leads to the rapid assembly of focal adhesion proteins and the formation of the complex between focal adhesion and actin filament bundle (Legerstee & Houtsmuller, 2021). After this, maturation of the focal contact begins, under the influence of physical and biochemical regulators (Zheng et al., 1998). During maturation, focal adhesions become larger and translocate towards the perinuclear region (Berginski et al., 2011).

Being complex macromolecular assemblies, FAs include approximately 232 various cytoplasmic molecules (Byron et al., 2016), including adaptor proteins (e.g., zyxin and paxillin), actin-associated proteins (e.g., talin, vinculin, α-actinin), GTPases, and enzymes such as tyrosine kinases (e.g., FAK (focal adhesion kinase) and Src), phosphatases, proteases, and lipases (Geiger et al., 2001; Kanchanawong et al., 2010; Wehrle-Haller, 2002).

One of the structural models of FAs is based on data from 3D super-resolution fluorescence iPALM microscopy (interferometric photoactivated localization microscopy) (**Fig. 2**). According to this model, FA is a multilayer structure, the outer layer of which consists of transmembrane integrin receptors, followed by a layer containing the cytoplasmic domains of integrins, focal contact kinase and paxillin. The next layer contains talin and vinculin; the top one is actin-regulating layer containing zyxin, VASP and α-actinin (Kanchanawong et al., 2010).

Integrins are transmembrane receptors consisting of α-β-heterodimers (Hynes, 2002). For mammals, 18 types of α- and 8 types of β-subunits are known, which form 24 types of integrins that can specifically recognize different types of ECM (Arnaout et al, 2007; Kuo, 2014). Integrin receptors are divided into 4 groups, namely: Arg-Gly-Asp (RGD)-binding integrins, which recognize the RGD sequence of the extracellular matrix (fibronectin, vitronectin, fibrinogen); Leu-Asp-Val (LDV) binding integrins that recognize the LDV motif in vascular cell adhesion molecule (MAdCAM-1) and intercellular cell adhesion molecule (ICAM-1); integrins containing the A domain that are able to interact with laminin and collagen; integrins that bind to laminin and lack an αA domain (**Table 1**).

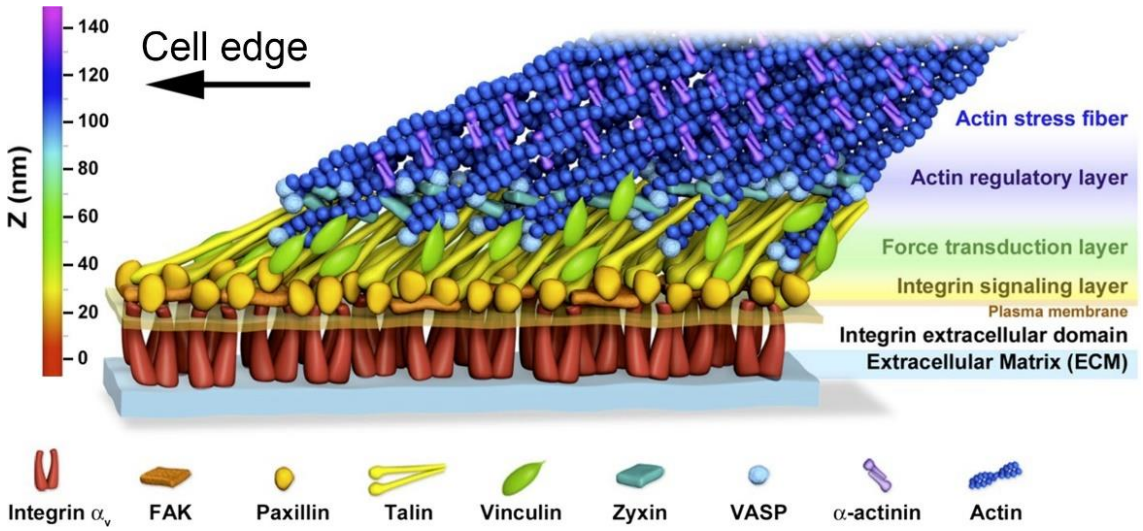

Figure 2. Schematic representation of the FA molecular structure using iPALM imaging, displaying 40 nm FA core region that separates integrins and actin, with multiple partially overlapping protein-specific strata (Kanchanawong et al., 2010)

Table 1. Four different classes of integrin receptors (Kuo, 2014)

Class	Name
RGD-binding integrins	αVβ1, αVβ3, αVβ5, αVβ6, αVβ8, αIIbβ3, α5β1, α8β1
LDV-binding integrins	α4β1, α4β7, αXβ2, αEβ7, α9β1, αLβ2, αDβ2, αMβ2
A domain-containing integrins	α1β1, α2β1, α10β1, α11β1
Non-αA domain-containing integrins	α3β1, α6β1, α7β1, α6β4

Depending on the affinity of integrin receptor to ECM components, ECM can exhibit varying adhesive properties, ranging from low to high adhesiveness. For instance, the interaction between the α5β1 integrins and fibronectin complex typically demonstrates stronger adhesive properties compared to the interaction between the α4β1 integrins and the cell adhesion molecule VCAM-1 (Humphries et al., 2009).

In the inactive state, the α and β subunits of integrins are linked to each other both extra- and intracellularly (Askari et al., 2010). Activation of integrins occurs upon interaction with an ECM ligand, resulting in the formation of integrin clusters, and subsequent divergence of the cytoplasmic domains of the α and β subunits. The FERM domain of talin binds to the NPXY motif of the integrin β-subunit, thereby enhancing the affinity of the integrin β-subunit for the ECM

ligand and promoting further clustering of integrin receptors (Theodosiou et al., 2015; Calderwood et al., 2013). Moreover, talin possesses two actin-binding sites and multiple vinculin binding sites (VBS) (Calderwood et al., 2013). Concurrently with talin, another protein, kindlin, can bind to the β-subunit of integrin, further promoting clustering and consequent activation of integrins (Ye et al., 2013).

Vinculin, which in the inactive state adopts a closed conformation, interacts with talin: the head N domain of vinculin, which has a D1 motif, hydrophobically binds to the VBS site of talin (Bakolitsa et al., 2004). This binding event activates vinculin, inducing a conformational change where the D1 motif moves inside the VBS domain. The binding of activated vinculin to talin promotes further clustering of integrins, thereby stimulating FA growth (Golji et al., 2011). Additionally, the N-domain of vinculin contains binding sites for α-actinin, while regions of the C-domain interact with actin and paxillin (Winkler et al., 1996). The central region of the vinculin molecule, enriched in proline residues, contains binding sites for Arp2/3. Following vinculin binding to talin, paxillin is recruited to FAs. Notably, this recruitment is not dependent on the presence of a paxillin-binding site in the C-domain of vinculin (Humphries et al., 2014).

Paxillin plays a crucial role in signal transmission between integrins and the small GTPase RhoA, facilitated by its four LIM domains (Smith et al., 2013). At its N-terminus, paxillin possesses five LD domains that mediate its interactions with various proteins, including vinculin, and FAK (Smith et al., 2013). The role of zyxin in FA composition remains somewhat ambiguous. While it is considered a key structural protein within FAs (Beningo et al., 2001), it also serves as a marker for mature focal contacts only (Zaidel-Bar et al., 2003). α-actinin is better known as an actin-binding protein, but it is capable of binding to the cytoplasmic tails of integrins (Liu et al., 2002), which ensures its inclusion in the FA. FAK is a tyrosine kinase that regulates the assembly and disassembly of FA by interacting with paxillin (Kwong et al., 2003).

1.2 Dynamics of focal adhesions

Based on wide heterogeneity in subcellular localization, size and molecular composition, FAs exhibit different types, including nascent adhesions, focal adhesions, fibrillar adhesions, podosomes, and 3D matrix adhesions (Geiger et al., 2001; Larsen et al., 2006). The development of adhesion structures usually begins with the formation of nascent FAs in the lamellipodia, approximately 1–2 μm from the leading edge, during cell spreading and migration (Alexandrova et al., 2008). These nascent adhesions have a short lifespan, potentially lasting not more than 60 seconds, and can either disappear or grow into FAs behind the lamellipodia in a tension-dependent mechanism mediated by actin decorated with non-muscle myosin II (Choi et al., 2008). FAs are ellipsoid structures exhibit wide heterogeneity in size (0.5-10 um) and lifetime

(several minutes to several hours) (Beningo et al., 2001). Fibrillar adhesions are specialized structures involved in ECM remodeling and are located at the cell center (Geiger & Yamada, 2011).

It was revealed by time-lapse microscopy that the integral intensity of individual FAs exhibits changes over time following a bell-shaped plot with distinct periods of focal adhesion assembly, relative stability, and disassembly (Berginski et al., 2011).

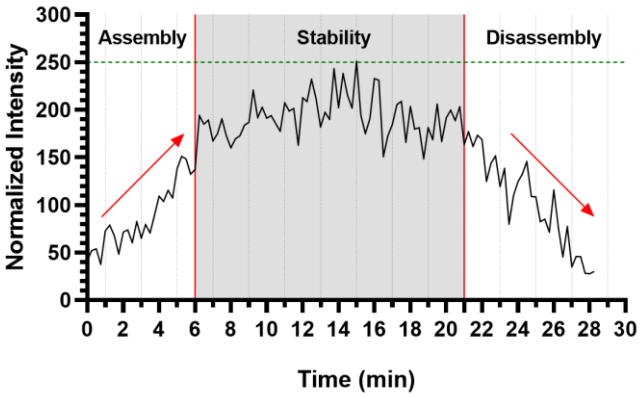

Figure 3. The intensity profile of individual FA labelled with vinculin-RFP through time with characteristic periods of assembly, stability, and disassembly. Intensity has been normalized to the intensity of cytoplasm by subtracting the median value of cytoplasmic background (preliminary data in concurrence with Berginski et al., 2011).

In the context of processive cell migration, a model cell is thought to actively generate new adhesions at the leading edge and stimulate disassembly of the FAs at the trailing edge (Vicente-Manzanares & Horwitz, 2011; **Fig. 2**). However, how and to what extent coordination of asymmetric FA dynamics and organization is achieved along the front-rear axis of a migrating cell is poorly understood.

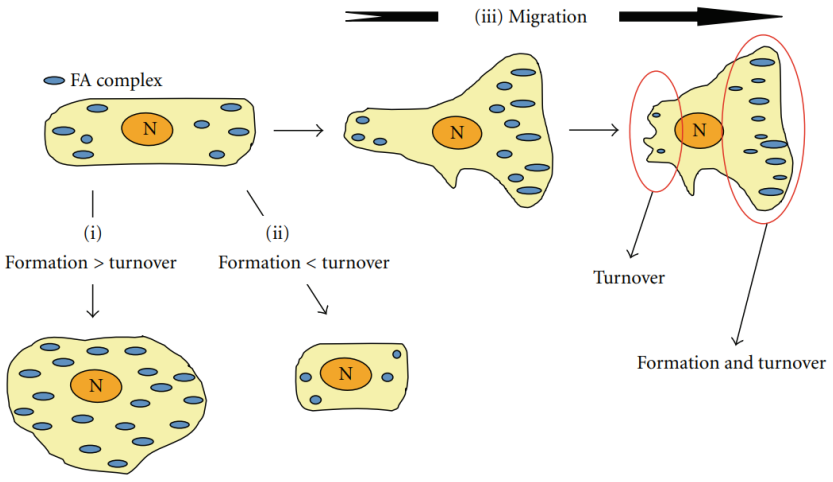

Figure 4. Model of asymmetrically regulated FA dynamics in directionally persistent migration, where the leading edge serves as the zone of active formation and turnover of FAs, while the trailing edge is the zone of FAs turnover (Nagano et al., 2012)

2. MATERIALS AND METHODS

2.1 Cell Culture and Reagents

A549 (ATCC, VA, USA) lung adenocarcinoma cells with stable vinculin-RFP (A549 VCL-RFP) expression obtained through lentiviral transduction, followed by sorting using a flow cytometry sorter were a gift from A. Saidova. A549 cells were grown in DMEM (Thermo Fisher Scientific, USA) supplemented with 8mM L-glutamine, 10% FBS, 100 U/ml penicillin and 100 ug/ml streptomycin (Thermo Fisher Scientific, USA). Cells were maintained in moist environment at 37°C in 5% CO2 incubator. 0.05% Trypsin-EDTA solution (Sigma-Aldrich, USA) was applied to detach cells from the surface of cell culture flasks. To reproduce cell migration on a physiological ECM substrate, glass chamber was coated with 5 ug/cm^2 fibronectin glycoprotein (Sigma-Aldrich, USA) prior cell seeding according to manufacturer's protocol.

2.2 Image acquisition

Cells were seeded in 8-well glass chamber (Ibidi, Germany) coated with fibronectin at 50-60% confluency and left overnight in CO_2 incubator at 37°C. The next day, the media in each well was changed to CO_2 media before image acquisition. All microscopic images were obtained from Zeiss Axio Observer microscope (Carl Zeiss AG, Germany) equipped with CSU-W1 Spinning Disk Unit (Yokogawa, Japan) and Prime 95B CMOS camera (Teledyne Photometrics, AZ, USA). Microscope is supplied with heating chamber unit (PeCon, Germany) and Metamorph software (Molecular Devices, CA, USA). Cell images were acquired in brightfield and fluorescent modes using Plan/Fluar x100/1.49 Oil objective with equivalent pixel size – 110 nm. All microscopy data was saved in .tif format files.

2.3 Data analysis

Image series were subjected to pre-processing using ImageJ open-source software (NIHImage, USA). Manual data analysis aimed at quantification of morphological and dynamic parameters of FAs was carried out in ImageJ software following the methodology described by Gladkikh et al. (2018). Life histories of individual focal adhesions were subjected to semi-manual analysis using kymographs (x-time representation depicting changes over time along FA track) build in ImageJ and processed using custom MATLAB (MathWorks, MA, USA) script.

2.4 Statistical analysis

The statistical analysis was conducted using Graphpad Prism software. Since datasets failed D'Agostino-Pearson omnibus normality test, nonparametric Kruskal-Wallis with Dunn's multiple

comparisons and Mann-Whitney U tests were used to compare independent samples (confidence interval 95%). Any observations more than 1.5 IQR below Q1 or more than 1.5 IQR above Q3 were excluded as outliers.

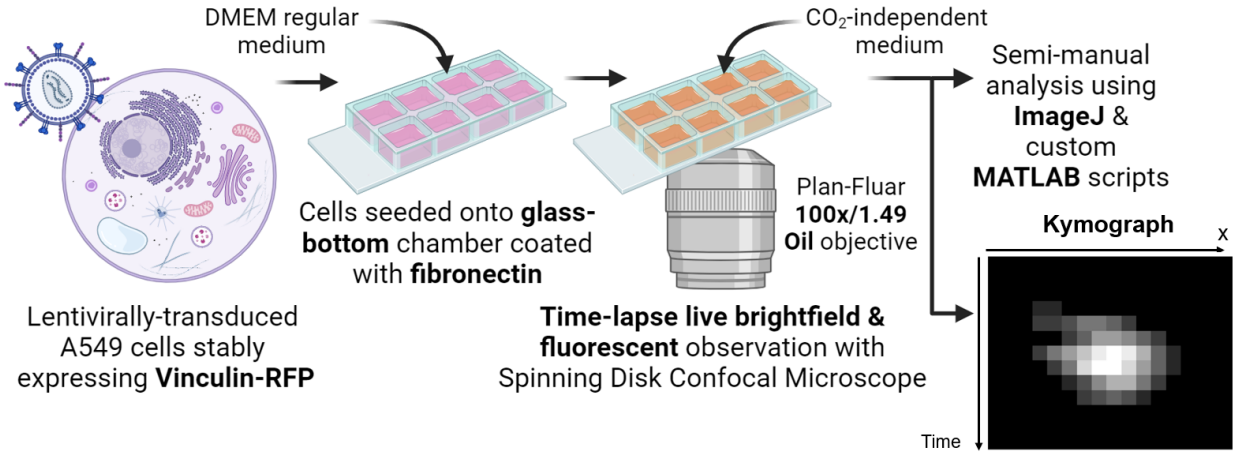

Figure 5. General outline of experimental procedures (Created in Biorender)

3. AIMS OF THE THESIS PROJECT

Since it remains elusive how considerable FA heterogeneity correlates with regional requirements to substrate adhesions intrinsic to cell migration, our aim was to identify and compare the dynamics of different FA populations at the two critical cell zones – leading and trailing edge. We aimed to analyze various morphodynamic parameters of FA, including localization, lifetime, size, frequency of formation, formation density, and translocation. To achieve this, we addressed the following set of questions:

- What populations of FAs are present on the leading and trailing cell edges, and how do they differ?
- How do the life histories and morphodynamic parameters of FAs differ at the leading and trailing cell edges?
- What is the origin and fate of FAs at the trailing edge?
- Do neighbouring FAs interact, and if so, does this interaction impart emergent properties to the resulting structures?

4. RESULTS

4.1 Asymmetry in focal adhesion dynamics

Most new adhesions formed within 2 μm from the edge of a protruding lamellae, with the majority disassembling within several minutes and some growing to form larger mature FAs with longer lifespan and higher integral intensity (**Fig. 6, 15**). Most FAs present at the trailing edge originated within lateral protrusions and only few of them formed directly there (**Fig. 17**). At a single moment in time, numerous small adhesions were observed at the leading edge, while only a few large adhesions were present of the trailing edge (**Fig. 6**).

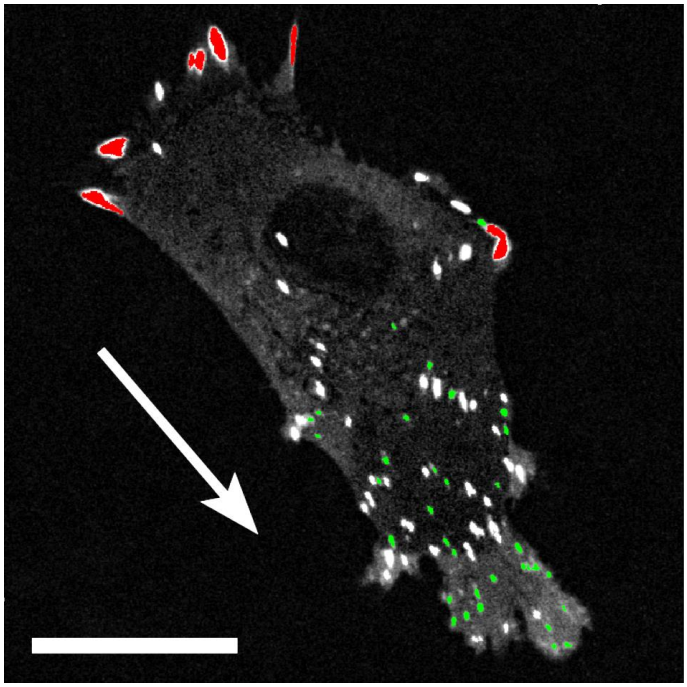

Figure 6. Snapshot of a migrating A549 cell with the smallest (<40th perc., green) and the largest FAs (>90th perc., red) marked. Scale bar: 20 μm.

4.2 Oscillating focal adhesions

It is anticipated that mature FAs would display characteristic sequence of assembly, stability, and disassembly (Berginski et al., 2011). The intensity and size profiles of most FAs indeed exhibited this sequential pattern, characterized by bell-shaped curves plotted over changes in intensity or size (**Fig. 7 A-C**). This overall trend was consistent across most FAs, despite that duration of assembly and disassembly phases may vary. However, a subset of FAs displayed an alternate behavior, featuring significant oscillations in intensity and size parameters over time (**Fig. 7 D**).

A)

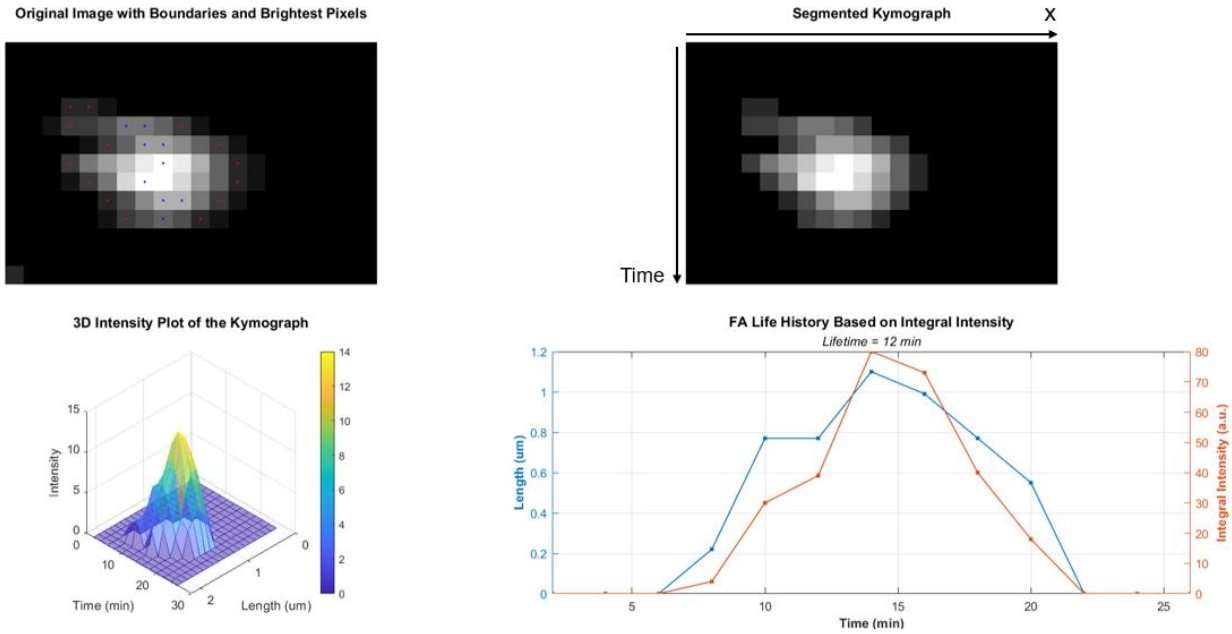

B)

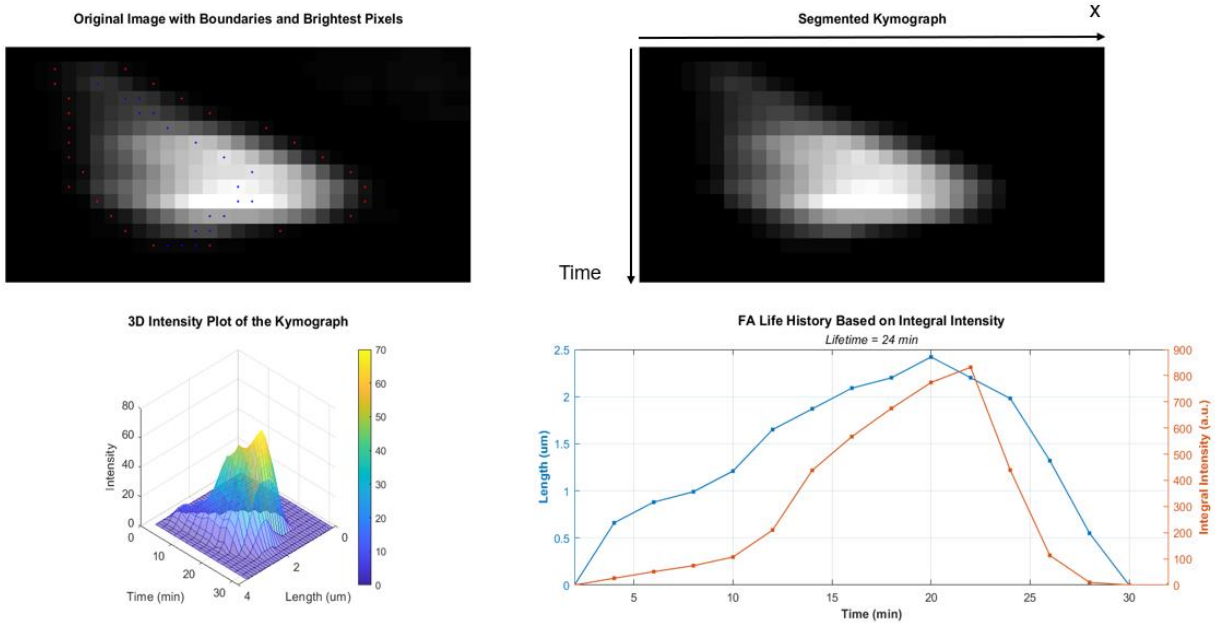

Figure 7. Output generated by custom MATLAB script for FA kymograph analysis. The upper panels display the results of kymograph segmentation with time on the vertical axis (each pixel equals 2 min) and distance along the horizontal axis (each pixel equals 110 nm). The lower panels display the 3D intensity plot of the kymograph (left) and FA life history based on integral brightness and length (as a proxy for size) changes (right). (A) FA with equal durations of assembly and disassembly; (B) FA with assembly longer than disassembly; (C) FA with assembly shorter than disassembly; (D) FA with oscillations in integral brightness and length.

C)

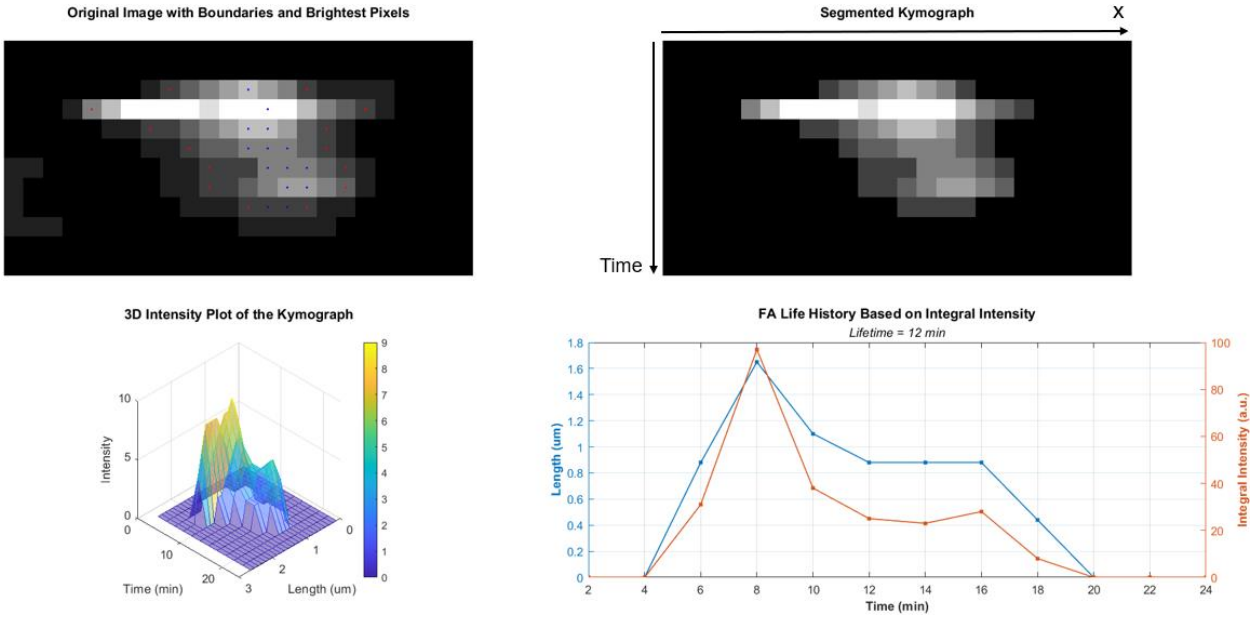

D)

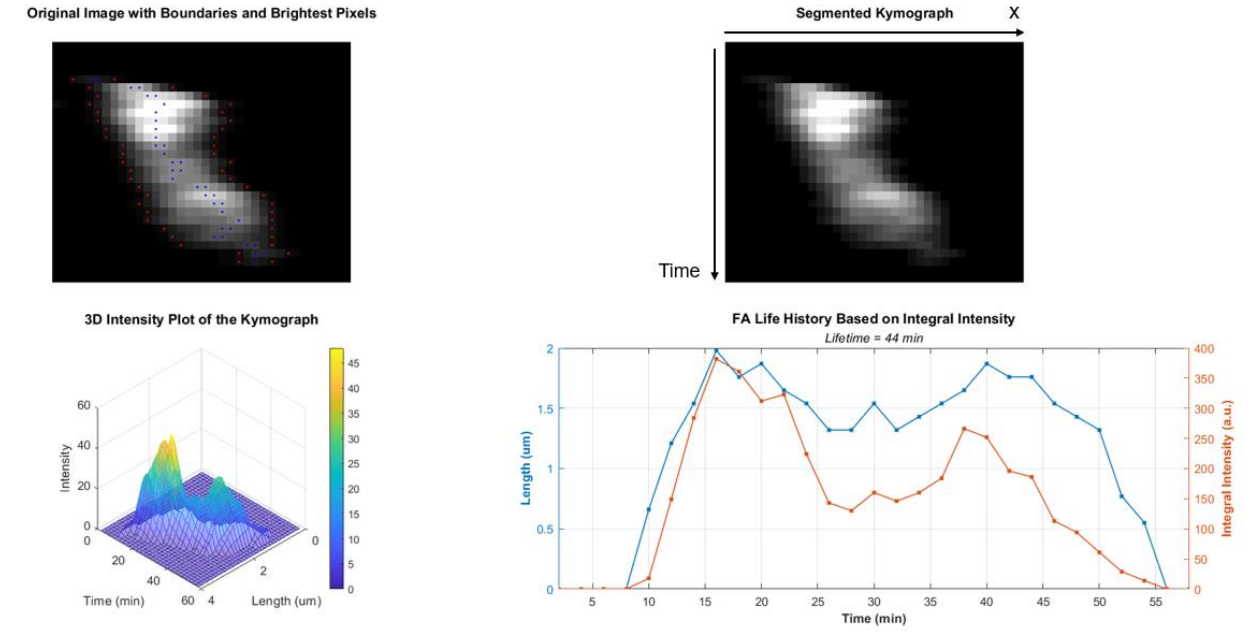

Having the periods of intermittent phases of partial disassembly and assembly in these oscillating FAs comparable in duration to those of initial assembly and final disassembly, these oscillating FAs exhibited significantly higher stability (longer lifespan) compared to other FA types (**Fig. 8**), while being not different in maximal integral intensity and maximal major axis length compared to other FA types (as a proxy for size; **Fig. 9**).

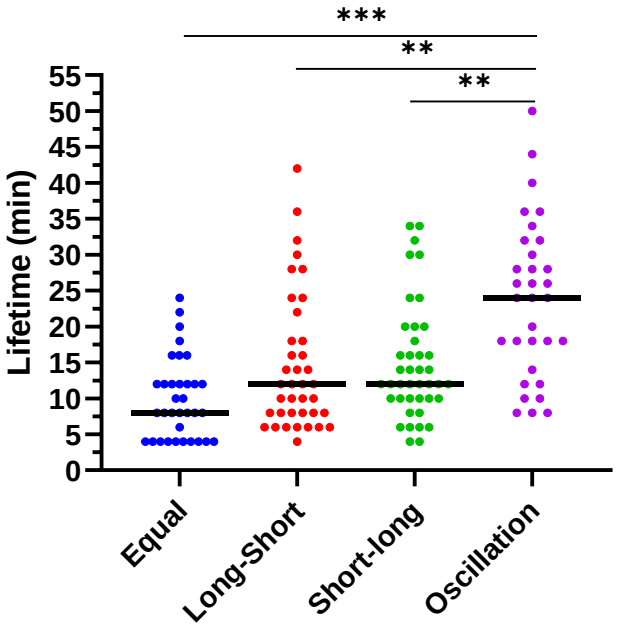

Figure 8. Lifetimes of four classes of individual FAs based on life histories at the leading edge of A549 cells. Equal – FAs with equal durations of assembly and disassembly, Long-Short – FAs with assembly longer than disassembly, Short-Long – FAs with assembly shorter than disassembly, Oscillation – FAs with oscillations in integral brightness and length. n = 145 FAs, 10 cells. Kruskal-Wallis test, Dunn's multiple comparisons. **p<0.01, ***p<0.001.

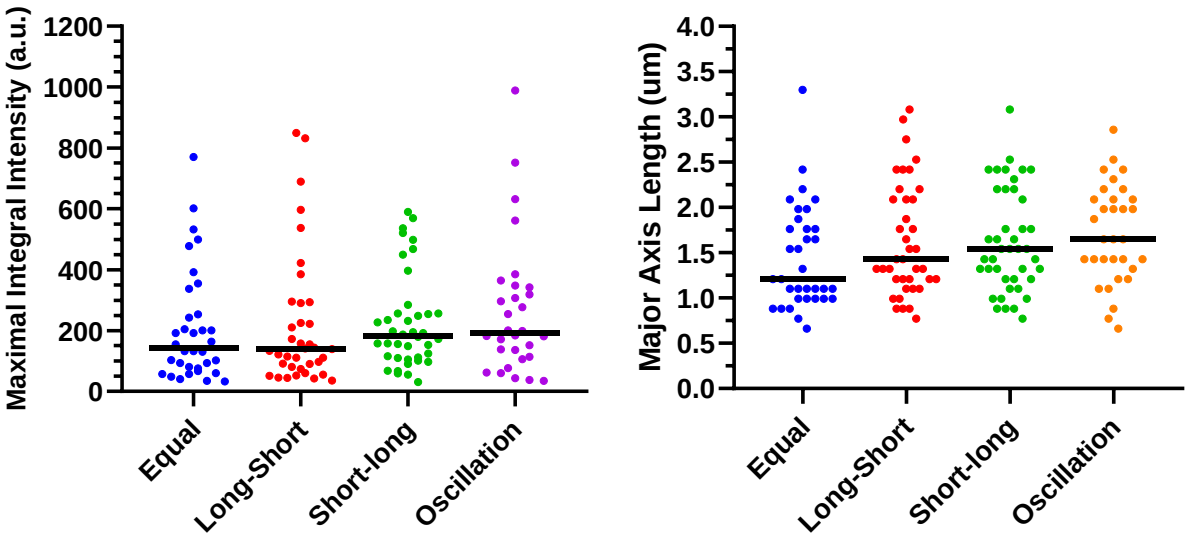

Figure 9. *Left*: Maximal integral intensity (in arbitrary units) of four classes of individual FAs based on life histories at the leading edge of A549 cells. n = 141 FAs, 10 cells. Kruskal-Wallis test, Dunn's multiple comparisons revealed no significant differences between groups. *Right*: Major axis length (um) of four classes of individual FAs based on life histories at the leading edge of A549 cells. Equal – FAs with equal durations of assembly and disassembly, Long-Short – FAs with assembly longer than disassembly, Short-Long – FAs with assembly shorter than disassembly, Oscillation – FAs with oscillations in integral brightness and length. n = 147 FAs, 10 cells. Kruskal-Wallis test, Dunn's multiple comparisons revealed no significant differences between groups.

4.3 Clusterization of focal adhesions

We have also observed another alteration from the typical assembly-stability-disassembly dynamics. Namely, some FAs formed clusters through merging with neighbouring FAs (**Fig. 10**).

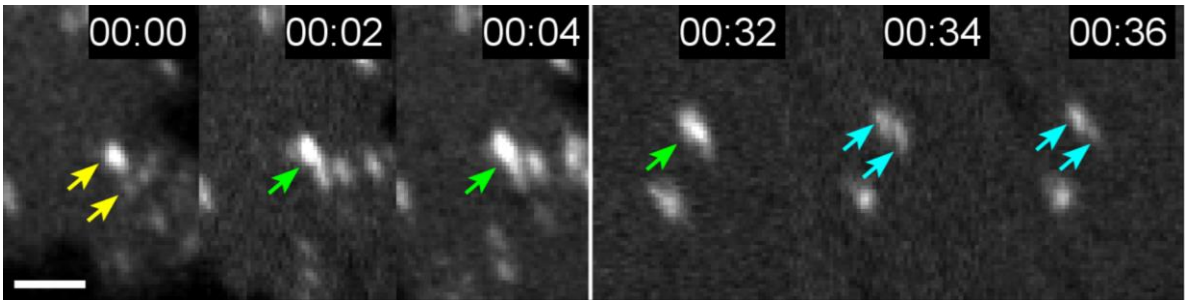

Figure 10. *Left*: Formation of a cluster at the leading edge through merging of two individual FAs. *Right***:** Cluster splitting into two daughter FAs. Scale bar: 5 µm.

Clusters were notably more frequent at the trailing edge (47%) than at the leading edge (6%; **Fig. 11**). Nevertheless, the formation density of clusters (1.53 events/100µm²/10min for the leading edge, 0.98 events/100µm²/10min for the retracting edge) was similar for both edges (**Fig. 12**) while leading edges demonstrate a higher formation density of individual FAs (19.29 events/100µm²/10min) compared to the trailing edges (2.04 events/100µm²/10min).

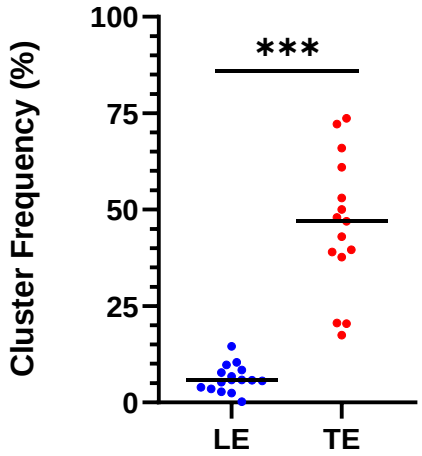

Figure 11. Cluster formation frequency (%) relative to the total formation events (clusters and individual FAs included). Clusters were notably more frequent at the trailing edge (47%) than at the leading edge (6%). n=15 in each group. Mann-Whitney test, ***p<0.001.

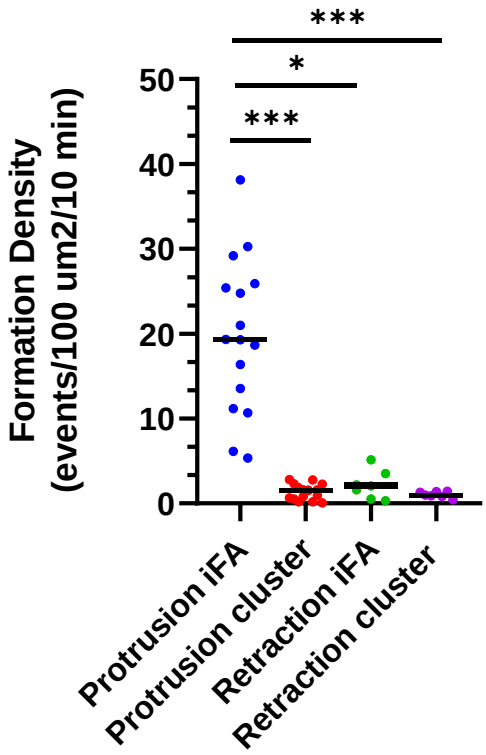

Figure 12. Cluster and individual FA formation density (events/100 um^2/10 min). Kruskal-Wallis test, Dunn's multiple comparisons. *p<0.05, **p<0.01, ***p<0.001.

After merging, a cluster might have further merge with neighbouring FAs, or split into "daughter" adhesions. The most complex cluster life histories were observed at the trailing edge, where, some FAs were growing, either through gradual increase in area and intensity or by merging with neighboring FAs, forming long-living FA clusters. These clusters might then further merge with neighbors or split, continuing their life as descendant FAs of an initial cluster from tens of minutes to several hours. To account for this dynamic remodeling of FA clusters and create the basis for their quantitative analysis, we propose the novel unit of analysis – cluster trees (**Fig. 13**).

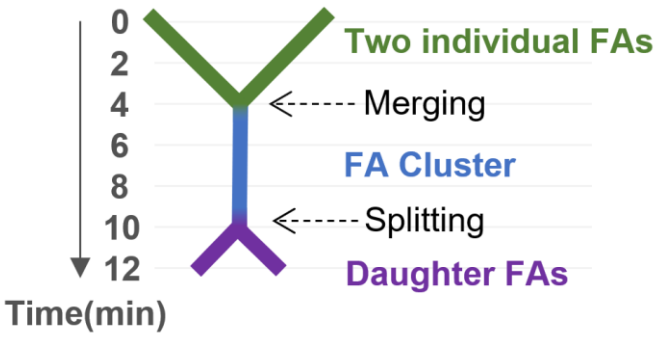

Figure 13. The scheme of a basic cluster tree, displaying merging of two individual FAs and subsequent splitting of a cluster into two daughter FAs. The lifetime of this cluster is 12 min.

Applying this novel unit, we compared the lifetimes of individual FAs and clusters at the leading and trailing edges (**Fig. 14**). Individual FAs' lifetime was significantly shorter than that of clusters, while there was no difference in the lifetimes of individual FAs at the leading and trailing edges (median 12 min). Clusters at the trailing edge lived considerably longer than clusters at the leading edge with median lifetimes 37 min and 20 min, respectively. The minimal and maximal lifetimes ranged from 6 min to 92 min for the leading edge, and from 4 min to 154 min for the trailing edge.

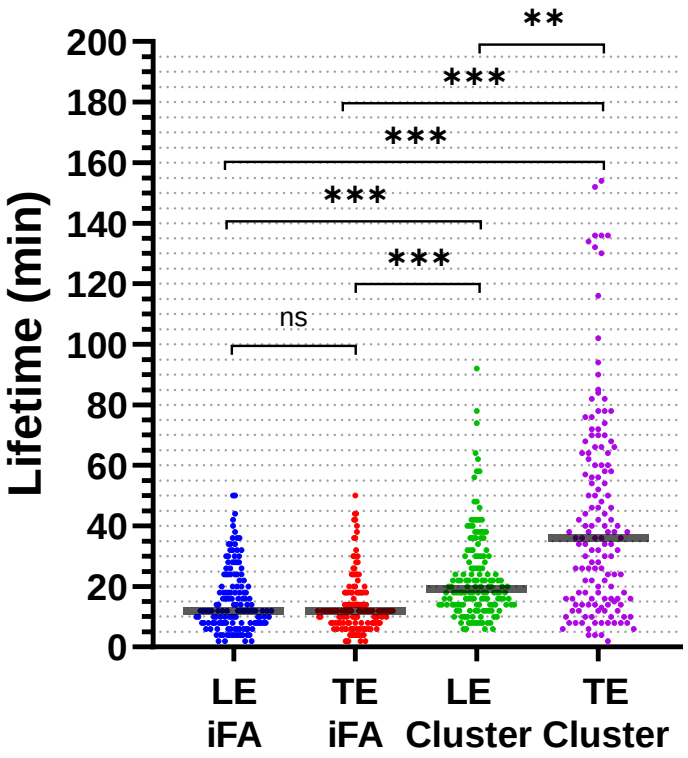

Figure 14. Lifetimes of individual FAs (iFA) and clusters at the leading edge (LE) and trailing edge (TE) of A549 cells, n = 150 FAs of each type, 10 cells. Kruskal-Wallis test, Dunn's multiple comparisons. **p<0.01, ***p<0.001.

4.4 Behaviour of focal adhesions during retraction of the rear cell edge

We also hypothesized that fates and disassembly of FAs at the trailing and leading edges might be regulated differently. During retraction of the rear cell edge, a portion of FAs has already been disassembled before retraction has reached them. However, some FAs at the trailing edge were enlarging, either through merging with neighboring FAs or gradual increase in area and intensity as they slid along with the trailing edge relative to the substrate. As a result, relatively large FAs were forcibly detached and rapidly disassembled only upon retraction edge reached them (**Fig. 15**).

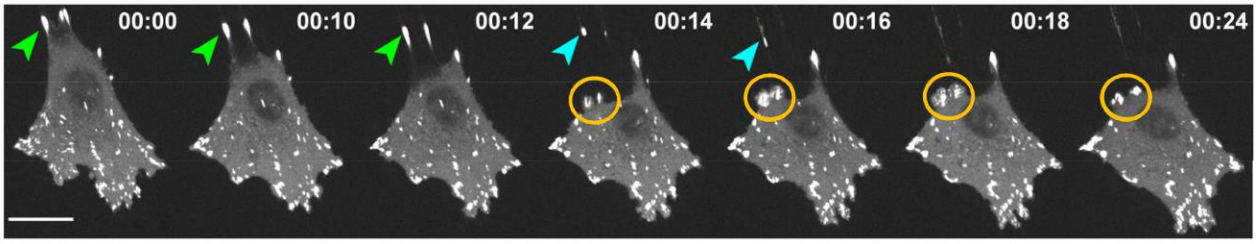

Figure 15. Forced retraction of FAs at the trailing edge in migrating A549 cell (green and cyan arrows). posterior protrusion generating new FAs at the trailing edge (yellow ellipses). Interframe interval 2 min. Scale bar: 20 um.

4.5 Translocation of focal adhesions

The last hypothesis has been that to provide mechanical anchorage necessary of cell advancement, FAs remain stationary over their lifetime. Surprisingly, we have observed that some FAs in the lamellae and cell body exhibited negligible translocation, while FAs at the trailing edge frequently slid to a considerable distance along with the trailing edge relative to the substrate without disassembly (**Fig. 16**). Moreover, we observed significantly longer lifespan of FAs that exhibited translocation for at least 1 μm (a value corresponding to a major axis length of an average FA) compared to stationary FAs (**Fig. 17**).

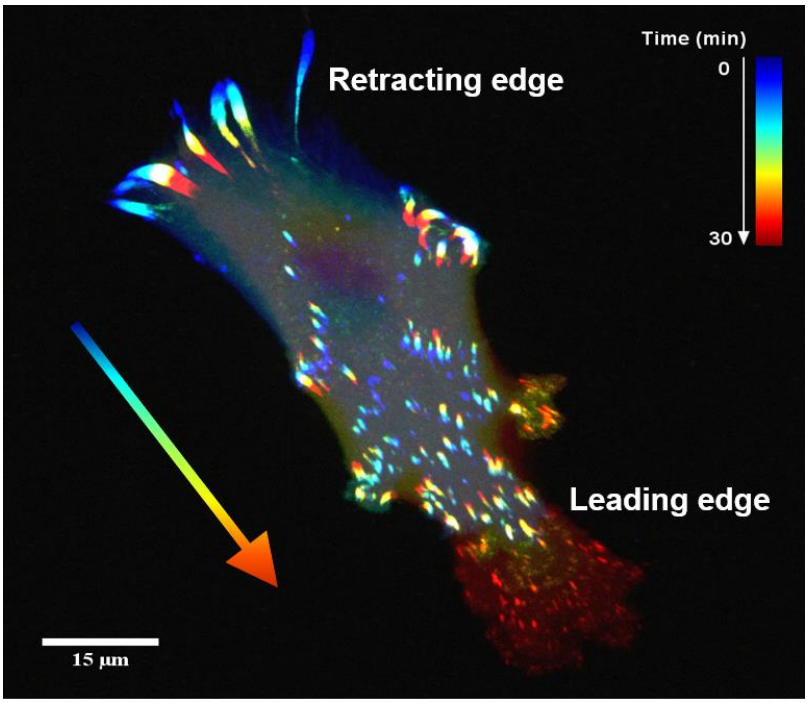

Figure 16. Color-coded time-lapse of A549 cell migration. Dynamic migration of is depicted over time, visually coded from blue (older) to red (newer regions) using a rainbow spectrum corresponding to the duration of the time-lapse recording (30 min). Both leading and trailing edges are clearly distinguishable. Scale bar: 15 μm. The figure was created with the Time Lapse Color Coder plugin in ImageJ.

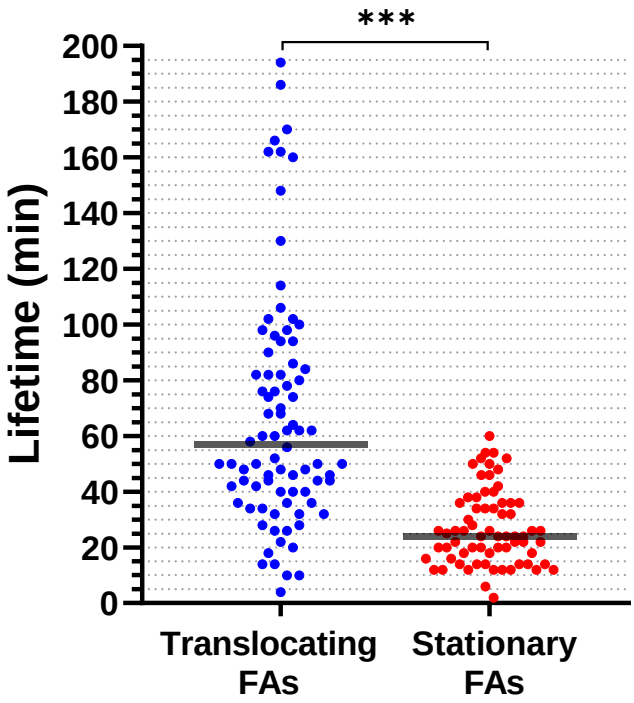

Figure 17. Lifetimes of FAs that translocated for more than 1 μm (n = 84) and that were stationary (n = 68) in A549 cell line, 5 cells. Kruskal-Wallis test, Dunn's multiple comparisons. *** $p<0.001$.

5. DISCUSSION

To evaluate FA dynamics, we employed live cell time-lapse spinning disc confocal microscopy with high spatial and temporal resolution, tracking FA size, lifetime, intensity, frequency of formation and localization in cancer A549 stably expressing vinculin-RFP. A549 lung carcinoma cells originate from epithelial tissues, yet have acquired mesenchymal characteristics, allowing them to actively migrate in vitro culture.

Vinculin was chosen as a target for FA visualization because it is recruited early in the formation of nascent FA and serves as a key structural protein within the central layer of the FA (Dumbauld et al., 2010). Alongside talin, vinculin contributes to the formation and maintenance of FAs by linking integrins to the actin stress fibers (Humphries et al., 2007). As a linker protein, vinculin offers a more conservative choice as a marker for FAs compared to integrins, which form variable heterodimeric complexes in different types of FAs (Iwamoto & Calderwood, 2015). Overall, vinculin allows for a comprehensive investigation of the morphology and dynamics of different FA types, facilitated by extensive research into its structure, functional and regulatory roles (Carisey & Ballestrem, 2011; Nagasato et al., 2017).

We observed FA dynamics using a model of random walk of cells on a rigid 2D substrate coated with ECM glycoprotein fibronectin. This matrix glycoprotein is known to be ubiquitously distributed throughout the interstitial matrix and is accumulated near the basement membrane (Miner, 2010). Despite the prevalence of 3D migration in physiological contexts (Yamada & Sixt, 2019), certain physiological processes, such as organogenesis and epithelial wound healing involve a form of collective migration along 2D sheets of basement membranes (Bindschadler & McGrath, 2007; Fisher & Rittié, 2017; Hsu et al., 2013). Additionally, the presence of FAs during 3D migration becomes context-dependent, influenced by the specific migratory mode adopted — whether collective, or individual, mesenchymal, lobopodial, or amoeboid (Merino-Casallo et al., 2022; Yamada & Sixt, 2019). Overall, while it is recognized that FAs display high adaptability to various migratory strategies observed in complex physiological environments (Yamada & Sixt, 2019), in vitro 2D migration model offers a controlled and reproducible environment for cell locomotion (Harunaga & Yamada, 2011).

Once anchored in the adhesive substrate, cells should push themselves forward or backward along the ECM using focal contacts (Chen et al., 2003). Indeed, we have found that the protruding lamellae are the main pool of newly formed FAs that undergo rapid turnover. It has been proposed that once cells have chosen the direction of migration, those focal contacts that have formed, as the cell body moves, eventually localize to the region of the lagging “tail” of the cell, where they are subsequently disassembled (Small et al., 2002). Alternatively, we observed that the trailing edge exhibited limited frequency of formation of new FAs. Most FAs observed at the trailing edge

originated within lateral protrusions, with only a few forming directly at this region. Moreover, it remains unclear, to what extent a cell is able to regulate the disassembly of FAs at the cell rear, since relatively large FAs were forcibly detached upon retraction edge reached them.

The investigation into whether FA cluster formation is a specific aspect in regional FA regulation and whether this characteristic imparts emergent properties or arises through spontaneous aggregation is of particular interest. Furthermore, it is crucial to explore how the persistence and remodeling of large translocating FAs at the trailing edge contribute to the reorganization of the actin cytoskeleton, as it may play a role in defining an axis coordinating directional migration (Petrie et al., 2009). Mathematical modeling might be used to determine the minimal set of regulatory mechanisms necessary to explain the wide heterogeneity in FA dynamics and organization, both within a single cell and across different cell lines.

Although it remains elusive how FA translocation is achieved mechanistically, we propose that translocation presents as another important characteristic that might predict FA longevity through a non-muscle myosin II decorated actin tension cues also related to the growth and maturation of nascent adhesions at the leading edge, as well as explain the longevity of large FAs at the trailing edge (Choi et al., 2008). The longer lifespan of oscillating FAs also might suggest an adaptable mechanism for sustaining prolonged anchorage while adhering to regional constraints on maximal size and protein density in FAs.

6. CONCLUSION

We have found that discernible disparity between the dynamics and organization of FAs emerges across different cell regions, particularly, leading and trailing edges. The leading edge, particularly protruding lamellae, was actively involved in the formation of new FAs, thus, constituting the primary source of FAs within a cell. Dynamic remodeling, involving merging, splitting, and translocation of FAs at trailing edge facilitated the displacement of the cell rear. Moreover, disassembly of FAs at the rear edge before retraction was not a prerequisite to edge retraction. FA translocation is most prominent at the cell rear and might predict FA longevity.

Hence, we propose that the extant set of FA parameters is insufficient to fully capture the diverse behaviors and morphologies exhibited by FAs. Additional metrics, namely oscillation, merging, splitting, translocation, and retraction of FAs, should be introduced to complement the existing set. These new metrics might help outline alternative mechanisms of regional FA regulation, thereby reinforcing the analytical framework for a more comprehensive understanding of FA dynamics.

REFERENCE LIST

Alexandrova, A. Y., Arnold, K., Schaub, S., Vasiliev, J. M., Meister, J.-J., Bershadsky, A. D., & Verkhovsky, A. B. (2008). Comparative Dynamics of Retrograde Actin Flow and Focal Adhesions: Formation of Nascent Adhesions Triggers Transition from Fast to Slow Flow. *PLoS ONE, 3*(9), e3234. doi:10.1371/journal.pone.0003234

Arnaout, M. A., Goodman, S. L., & Xiong, J.-P. (2007). Structure and mechanics of integrin-based cell adhesion. *Current Opinion in Cell Biology, 19*(5), 495–507. doi:10.1016/j.ceb.2007.08.002

Askari, J. A., Tynan, C. J., Webb, S. E. D., Martin-Fernandez, M. L., Ballestrem, C., & Humphries, M. J. (2010). Focal adhesions are sites of integrin extension. *The Journal of Cell Biology, 188*(6), 891–903. doi:10.1083/jcb.200907174

Bakolitsa, C., Cohen, D. M., Bankston, L. A., Bobkov, A. A., Cadwell, G. W., Jennings, L., … Liddington, R. C. (2004). Structural basis for vinculin activation at sites of cell adhesion. *Nature, 430*(6999), 583–586. doi:10.1038/nature02610

Beningo, K. A., Dembo, M., Kaverina, I., Small, J. V., & Wang, Y. (2001). Nascent Focal Adhesions Are Responsible for the Generation of Strong Propulsive Forces in Migrating Fibroblasts. *The Journal of Cell Biology, 153*(4), 881–888. doi:10.1083/jcb.153.4.881

Berginski, M. E., Vitriol, E. A., Hahn, K. M., & Gomez, S. M. (2011). High-Resolution Quantification of Focal Adhesion Spatiotemporal Dynamics in Living Cells. *PLoS ONE, 6*(7), e22025. doi:10.1371/journal.pone.0022025

Bindschadler, M., & McGrath, J. L. (2007). Sheet migration by wounded monolayers as an emergent property of single-cell dynamics. *Journal of Cell Science, 120*(5), 876–884. doi:10.1242/jcs.03395

Byron, A., & Frame, M. C. (2016). Adhesion protein networks reveal functions proximal and distal to cell-matrix contacts. *Current Opinion in Cell Biology, 39*, 93–100. doi:10.1016/j.ceb.2016.02.013

Calderwood, D. A., Campbell, I. D., & Critchley, D. R. (2013). Talins and kindlins: partners in integrin-mediated adhesion. *Nature Reviews Molecular Cell Biology, 14*(8), 503–517. doi:10.1038/nrm3624

Carisey, A., & Ballestrem, C. (2011). Vinculin, an adapter protein in control of cell adhesion signalling. *European Journal of Cell Biology, 90*(2-3), 157–163. doi:10.1016/j.ejcb.2010.06.007

Choi, C. K., Vicente-Manzanares, M., Zareno, J., Whitmore, L. A., Mogilner, A., & Horwitz, A. R. (2008). Actin and α-actinin orchestrate the assembly and maturation of nascent adhesions in a myosin II motor-independent manner. *Nature Cell Biology, 10*(9), 1039–1050.

https://doi.org/10.1038/ncb1763

Cukierman, E., Pankov, R., Stevens, D. R., & Yamada, K. M. (2001). Taking cell-matrix adhesions to the third dimension. *Science*, *294*(5547), 1708–1712. https://doi.org/10.1126/science.1064829

Dumbauld, D. W., Shin, H., Gallant, N. D., Michael, K. E., Radhakrishna, H., & García, A. J. (2010). Contractility modulates cell adhesion strengthening through focal adhesion kinase and assembly of vinculin-containing focal adhesions. *Journal of Cellular Physiology*, *223*(3), 746–756. https://doi.org/10.1002/jcp.22084

Fisher, G., & Rittié, L. (2017). Restoration of the basement membrane after wounding: a hallmark of young human skin altered with aging. *Journal of Cell Communication and Signaling, 12*(1), 401–411. doi:10.1007/s12079-017-0417-3

Friedl, P., & Gilmour, D. (2009). Collective cell migration in morphogenesis, regeneration and cancer. *Nature Reviews Molecular Cell Biology, 10*(7), 445–457. doi:10.1038/nrm2720

Geiger, B., & Yamada, K. M. (2011). Molecular Architecture and Function of Matrix Adhesions. *Cold Spring Harbor Perspectives in Biology, 3*(5), a005033–a005033. doi:10.1101/cshperspect.a005033

Geiger, B., Bershadsky, A., Pankov, R., & Yamada, K. M. (2001). Transmembrane crosstalk between the extracellular matrix and the cytoskeleton. *Nature Reviews Molecular Cell Biology*, *2*(11), 793–805. doi:10.1038/35099066

Gladkikh, A., Kovaleva, A., Tvorogova, A., & Vorobjev, I. A. (2018). Heterogeneity of focal adhesions and focal contacts in motile fibroblasts. In *Methods in Molecular Biology* (Vol. 1745, pp. 205–218). Humana Press Inc. https://doi.org/10.1007/978-1-4939-7680-5_12

Golji, J., Lam, J., & Mofrad, M. R. K. (2011). Vinculin Activation Is Necessary for Complete Talin Binding. *Biophysical Journal, 100*(2), 332–340. doi:10.1016/j.bpj.2010.11.024

Harunaga, J. S., & Yamada, K. M. (2011). Cell-matrix adhesions in 3D. *Matrix Biology, 30*(7-8), 363–368. doi:10.1016/j.matbio.2011.06.001

Hsu, J. C., Koo, H., Harunaga, J. S., Matsumoto, K., Doyle, A. D., & Yamada, K. M. (2013). Region-specific epithelial cell dynamics during branching morphogenesis. *Developmental Dynamics, 242*(9), 1066–1077. doi:10.1002/dvdy.24000

Humphries, J. D., Wang, P., Streuli, C., Geiger, B., Humphries, M. J., & Ballestrem, C. (2007). Vinculin controls focal adhesion formation by direct interactions with talin and actin. *Journal of Cell Biology, 179*(5), 1043–1057. https://doi.org/10.1083/jcb.200703036

Humphries, J. D., Byron, A., Bass, M. D., Craig, S. E., Pinney, J. W., Knight, D., & Humphries, M. J. (2009). Proteomic Analysis of Integrin-Associated Complexes Identifies RCC2 as a Dual Regulator of Rac1 and Arf6. *Science Signaling, 2*(87), ra51–ra51.

doi:10.1126/scisignal.2000396

Humphries, J. D., Wang, P., Streuli, C., Geiger, B., Humphries, M. J., & Ballestrem, C. (2007). Vinculin controls focal adhesion formation by direct interactions with talin and actin. *The Journal of Cell Biology, 179*(5), 1043–1057. doi:10.1083/jcb.200703036

Hynes, R. O. (2002). Integrins: Bidirectional, Allosteric Signaling Machines. *Cell, 110*(6), 673–687. doi:10.1016/s0092-8674(02)00971-6

Iwamoto, D. V., & Calderwood, D. A. (2015). Regulation of integrin-mediated adhesions. *Current Opinion in Cell Biology, 36*, 41–47. doi:10.1016/j.ceb.2015.06.009

Kanchanawong, P., Shtengel, G., Pasapera, A. M., Ramko, E. B., Davidson, M. W., Hess, H. F., & Waterman, C. M. (2010). Nanoscale architecture of integrin-based cell adhesions. *Nature, 468*(7323), 580–584. doi:10.1038/nature09621

Kuo, J.-C. (2014). Focal Adhesions Function as a Mechanosensor. *Mechanotransduction*, 55–73. doi:10.1016/b978-0-12-394624-9.00003-8

Kwong, L., Wozniak, M. A., Collins, A. S., Wilson, S. D., & Keely, P. J. (2003). R-Ras Promotes Focal Adhesion Formation through Focal Adhesion Kinase and p130Cas by a Novel Mechanism That Differs from Integrins. *Molecular and Cellular Biology, 23*(3), 933–949. doi:10.1128/mcb.23.3.933-949.2003

Larsen, M., Artym, V. V., Green, J. A., & Yamada, K. M. (2006). The matrix reorganized: extracellular matrix remodeling and integrin signaling. *Current Opinion in Cell Biology, 18*(5), 463–471. doi:10.1016/j.ceb.2006.08.009

Legerstee, K., & Houtsmuller, A. B. (2021). A layered view on focal adhesions. *Biology*, *10*(11). https://doi.org/10.3390/biology10111189

Liu, S., Kiosses, W. B., Rose, D. M., Slepak, M., Salgia, R., Griffin, J. D., … Ginsberg, M. H. (2002). A Fragment of Paxillin Binds the α4Integrin Cytoplasmic Domain (Tail) and Selectively Inhibits α4-Mediated Cell Migration. *Journal of Biological Chemistry, 277*(23), 20887–20894. doi:10.1074/jbc.m110928200

Mattila, P. K., & Lappalainen, P. (2008). Filopodia: molecular architecture and cellular functions. *Nature Reviews Molecular Cell Biology, 9*(6), 446–454. doi:10.1038/nrm2406

Maziveyi, M., & Alahari, S. K. (2017). Cell matrix adhesions in cancer: The proteins that form the glue. *Oncotarget, 8*(29). doi:10.18632/oncotarget.17265

Merino-Casallo, F., Gomez-Benito, M. J., Hervas-Raluy, S., & Garcia-Aznar, J. M. (2022). Unravelling cell migration: defining movement from the cell surface. *Cell Adhesion and Migration*. Taylor and Francis Ltd. https://doi.org/10.1080/19336918.2022.2055520

Miner, J. H. (2011). Basement membranes. In *The Extracellular Matrix: an Overview* (Vol. 1, pp. 117–145). Germany: Springer Berlin Heidelberg.

Nagano, M., Hoshino, D., Koshikawa, N., Akizawa, T., & Seiki, M. (2012). Turnover of Focal Adhesions and Cancer Cell Migration. *International Journal of Cell Biology*, 1–10. doi:10.1155/2012/310616

Nagasato, A. I., Yamashita, H., Matsuo, M., Ueda, K., & Kioka, N. (2017). The distribution of vinculin to lipid rafts plays an important role in sensing stiffness of extracellular matrix. Bioscience, *Biotechnology and Biochemistry*, *81*(6), 1136–1147. https://doi.org/10.1080/09168451.2017.1289074

Petrie, R. J., Doyle, A. D., & Yamada, K. M. (2009). Random versus directionally persistent cell migration. *Nature Reviews Molecular Cell Biology, 10*(8), 538–549. doi:10.1038/nrm2729

Prager-Khoutorsky, M., Lichtenstein, A., Krishnan, R., Rajendran, K., Mayo, A., Kam, Z., … Bershadsky, A. D. (2011). Fibroblast polarization is a matrix-rigidity-dependent process controlled by focal adhesion mechanosensing. *Nature Cell Biology, 13*(12), 1457–1465. https://doi.org/10.1038/ncb2370

Ridley, A. J. (2003). Cell Migration: Integrating Signals from Front to Back. *Science, 302*(5651), 1704–1709. doi:10.1126/science.1092053

Rooney, C., White, G., Nazgiewicz, A., Woodcock, S. A., Anderson, K. I., Ballestrem, C., & Malliri, A. (2010). The Rac activator STEF (Tiam2) regulates cell migration by microtubule-mediated focal adhesion disassembly. *EMBO Reports, 11*(4), 292–298. doi:10.1038/embor.2010.10

Scarpa, E., & Mayor, R. (2016). Collective cell migration in development. *The Journal of Cell Biology*, *212*(2), 143–155. doi:10.1083/jcb.201508047

Smith, M. A., Blankman, E., Deakin, N. O., Hoffman, L. M., Jensen, C. C., Turner, C. E., & Beckerle, M. C. (2013). LIM Domains Target Actin Regulators Paxillin and Zyxin to Sites of Stress Fiber Strain. *PLoS ONE, 8*(8), e69378. doi:10.1371/journal.pone.0069378

Theodosiou, M., Widmaier, M., Böttcher, R. T., Rognoni, E., Veelders, M., Bharadwaj, M., … Fässler, R. (2016). Kindlin-2 cooperates with talin to activate integrins and induces cell spreading by directly binding paxillin. *ELife, 5*. https://doi.org/10.7554/eLife.10130

Vicente-Manzanares, M., & Horwitz, A. R. (2011). Adhesion dynamics at a glance. *Journal of Cell Science, 124*(23), 3923–3927. https://doi.org/10.1242/jcs.095653

Wehrle-Haller, B. (2002). The inner lives of focal adhesions. *Trends in Cell Biology, 12*(8), 382–389. doi:10.1016/s0962-8924(02)02321-8

Winkler, J., Lünsdorf, H., & Jockusch, B. M. (1996). The Ultrastructure of Chicken Gizzard Vinculin as Visualized by High-Resolution Electron Microscopy. *Journal of Structural Biology*, *116*(2), 270–277. doi:10.1006/jsbi.1996.0042

Yamada, K. M., & Sixt, M. (2019). Mechanisms of 3D cell migration. *Nature Reviews Molecular*

Cell Biology, *20*(12), 738–752. doi:10.1038/s41580-019-0172-9

Ye, F., Petrich, B. G., Anekal, P., Lefort, C. T., Kasirer-Friede, A., Shattil, S. J., … Ginsberg, M. H. (2013). The Mechanism of Kindlin-Mediated Activation of Integrin αIIbβ3. *Current Biology*, *23*(22), 2288–2295. doi:10.1016/j.cub.2013.09.050

Zaidel-Bar, R. (2003). Early molecular events in the assembly of matrix adhesions at the leading edge of migrating cells. *Journal of Cell Science, 116*(22), 4605–4613. doi:10.1242/jcs.00792

Zheng, C., Xing, Z., Bian, Z. C., Guo, C., Akbay, A., Warner, L., & Guan, J.-L. (1998). Differential Regulation of Pyk2 and Focal Adhesion Kinase (FAK). *Journal of Biological Chemistry*, *273*(4), 2384–2389. doi:10.1074/jbc.273.4.2384